

Physical origin underlying the entropy loss upon hydrophobic hydration

Aljaž Godec^{1,*} and Franci Merzel^{1,†}

¹*National Institute of Chemistry, Hajdrihova 19, 1000 Ljubljana, Slovenia*

(Dated: June 18, 2018)

arXiv:1202.1228v1 [cond-mat.stat-mech] 6 Feb 2012

The hydrophobic effect (HE) is commonly associated with the demixing of oil and water at ambient conditions and plays the leading role in determining the structure and stability of biomolecular assembly in aqueous solutions. On the molecular scale HE has an entropic origin. It is believed that hydrophobic particles induce order in the surrounding water by reducing the volume of configuration space available for hydrogen bonding.

Here we show with computer simulation results that this traditional picture is not correct. Analyzing collective fluctuations in water clusters we are able to provide a fundamentally new picture of HE based on pronounced many-body correlations affecting the switching of hydrogen bonds between molecules. These correlations emerge as a non-local compensation of reduced fluctuations of local electrostatic fields in the presence of an apolar solute.

The HE has a multifaceted nature, *i.e.* its physical manifestation depends on the length-scale¹. On the mesoscale, *i.e.* hydration of an assembly of hydrophobic units or an extended hydrophobic surface, HE is driven by energy/enthalpy and occurs as a 'dewetting' transition²⁻⁴ which has far-reaching consequences for processes such as protein folding^{5,6} and nanoparticle self-assembly⁷. Meanwhile, HE on the molecular scale has an entropic origin^{1,8}, particularly near room temperature and lower, while it is believed to eventually become energy/enthalpy driven at higher temperatures^{9,10}. Furthermore, the molecular scale hydration thermodynamics (hydrophobe solubilities, partitioning of hydration free energy into energy/enthalpy and entropy contributions, etc.) appear to be well established and can be worked out, for example, using scaled-particle theory¹¹ or information theory¹². While those theories are successful in predicting solubilities of hydrophobic solutes and several related thermodynamic features, they do not provide deeper insight into the physical mechanism underlying HE. Notwithstanding all efforts and advances in the field^{1-4,8,11,13-15} the physical picture of HE is still far from being complete and even fundamental issues, such as the mechanism underlying hydrophobicity on different length scales, still have to be clarified. From the physical point of view the most puzzling feature of HE remains the microscopic picture of entropy loss upon hydrophobic hydration.

Intuitively, the entropy loss is usually attributed to the reduction of configuration space available for hydrogen-bonding^{1,8}, which is due to the fact that water molecules need to reorganize around a hydrophobic solute to avoid sacrificing hydrogen bonds. This is supposed

to lead to remnants of clathrate structures¹⁶, which are, however, not rigid and their quantitative importance for understanding hydrophobicity remains questionable¹⁵. Furthermore, even the actual role of hydrogen bonds for the HE is apparently not entirely clear^{10,17}.

Thus, the physically most intriguing question to be answered still remains: If HE is entropy driven, what specifically causes the loss of entropy? Since entropy loss is directly related to a reduction of available volume in configuration space, how does it affect degrees of freedom of water molecules?

Here we present conclusive simulation results which unravel a fundamentally new picture of the mechanism of HE based on pronounced many-body correlations affecting the intermolecular exchanging of hydrogen bonds. We carry out constant pressure Monte-Carlo simulations of TIP5P water¹⁸ and model hard sphere solutes in an orthogonal simulation box with periodic boundary conditions (see Methods section for details).

In order to present the conceptual change in our understanding of the HE we first address the inconsistencies of the traditional picture. The radial correlation function, $\frac{\rho(r)}{\rho_B} \equiv g(r) = \rho_B^{-1} \langle \sum_{i=1}^N \delta(r - |\mathbf{r}_i|) \rangle$, is used to quantify the degree of translational ordering of water molecules around hydrophobic solutes. We find a non-monotonic dependence of the contact density on particle size, which is due to commensurability of the solute surface and water packing. The relative density fluctuations monotonically decrease with solute size. Two water molecules are defined to be in close contact if their intermolecular distance is less than 3 Å, and they are said to be hydrogen-bonded if they are in close contact and if the angle $O - H \cdots O$ is larger than 150°. The cutoff distance for neighbors in close contact is set at 3 Å and is more appropriate with respect to the conventional definition of 3.5 Å¹⁹, as there is no preferential mutual orientation beyond the distance of 3 Å (see Fig. 2c). The distribution of the number of water molecules in close contact and the number of hydrogen bonded contacts per water molecule located in the first and second hydration shell and in bulk water is shown in Fig. 1b and c. Except for the smallest solute (with radius 1.4 Å) there is no appreciable difference (say of the order of ≥ 0.5) in the number of total and hydrogen-bonded contacts with respect to bulk water, neither in the first nor in the second hydration shell. If the main effect of a hydrophobic solute would be the reduction of the configuration space for hydrogen bonding, then one would naturally expect to find less neighbors in close contact. Clearly, this is not the case. Moreover, the distribution is much narrower in bulk water, which already suggests that the small-scale fluctuations in the

vicinity of hydrophobes (i.e. librations, hydrogen-bond exchange, etc.) are enhanced with respect to the bulk. According to our criterion for the nearest neighbor we find that the probability of a water molecule having 3 hydrogen-bonded nearest neighbors is negligible, irrespective of its position.

Aside from an altered number of nearest neighbors the traditional picture also suggest a more ordered local structure. In order to cause entropy loss the structural fluctuations should tend to diminish. To inspect in detail the structural ordering of water molecules in close contact, around hydrophobic particles and in bulk water, we employ the recently introduced dipolar order parameter²⁰,

$$D(i) = \frac{1}{N} \sum_{j=1}^N \left(\frac{\alpha_{ij} - \alpha_{ij}^{min}}{\alpha_{ij}^{max} - \alpha_{ij}^{min}} \right) \quad (1)$$

where $i \neq j$ and the sum is taken over the N neighbors in the first coordination shell of the i -th water molecule and α_{ij}^{max} and α_{ij}^{min} correspond to maximal and minimal dipole-dipole potential at a given intermolecular unit vector and unit dipole vector of the tagged molecule. This way, $D(i)$ takes values between 0 (maximal repulsion) and 1 (maximal attraction). The distributions of dipolar ordering shown in Fig. 2 confirm the idea that water is on average slightly more orientationally ordered in the first hydration shell of hydrophobic particles (note the slight shift of the distributions towards higher D values). More importantly, the width of the distributions $p(D)$, which reflects the constraining of orientational degrees of freedom, remains rather unaffected. This width clearly increases upon increasing polarity of the solute indicating an orientational relaxation in the hydrogen-bond network²⁰. The situation in the second shell is similar, albeit less pronounced. Most likely, due to a commensurability effect, the second shell molecules exhibit a reverse trend in orientational ordering in the case of s_2 .

Apparently the pair interactions and consequently also the hydrogen bonds are strengthened but there is no reduction of the orientational configuration space explored by individual water molecules in the hydration shells as the distributions are merely shifted while their form remains unchanged. Thus, we find that *i*) there are no significant differences in the number of nearest HB and non-HB neighbors and *ii*) there is no orientational constraining although the local structure is more ordered. This is clearly in contradiction with the idea of reduced configuration space available for hydrogen bonding^{1,8}. So how can this contradiction be reconciled?

There is an important difference between the total volume of configuration space and the volume that is actually visited at a given temperature. As the number of close contacts is not altered significantly by the mere presence of the solute the latter is not expected to significantly affect the volume of the configuration space available to a water molecule for hydrogen bonding. On the other hand, in the liquid state water molecules form a dynamic, labile hydrogen-bond network. There is clear evidence that the molecular reorientation underlying the exchange of hydrogen bonds is not diffusive (*i.e.* does not occur as angular Brownian motion) but rather proceeds in terms of large-amplitude sudden jumps^{19,21-26}. As it is impossible for water molecules to each form four HBs at a time in the liquid state, this introduces a strong frustration into the system emerging from the competition between the entropic and energetic driving forces. This means, that while fluctuating about the minimum energy configuration exhibiting *e.g.* librational movements, a water molecule is most likely to form two hydrogen-bonds to its closest neighbors. As a water molecule in the bulk liquid is intrinsically inclined to form more than one hydrogen bond, this necessarily leads to confinement of its orientational configuration space. This fact suggests to rationalize the entropy loss in HE in an alternative way.

The current understanding of hydrogen-bond network dynamics in neat water already anticipates the collective concerted motions of several water molecules²⁶. This suggests looking for the potential source of entropy loss in the altered 'communication' between emerging transient water clusters involved in the exchange of hydrogen bonds, *i.e.* the reduction of configuration space due to constraining of collective degrees of freedom. For large enough fluctuations the transient water cluster can rearrange into another configuration just by the exchange of hydrogen bonds. Hydrogen-bond fluctuations (for example, librations) try to compensate for the entropic frustrations caused by a transient mutual alignment of water molecules in between sudden jumps. Since structural fluctuations are caused by local field fluctuations they are expected to be dramatically suppressed in direct vicinity of a hydrophobic solute, because the latter exerts only an extremely weak electrostatic field. Without an additional compensation mechanism the hydrogen bonds would be significantly strengthened and the entropic frustrations would be expected to grow further. Therefore there must exist a tendency of nearby water molecules (nearest and next-nearest neighbors) to compensate for the suppressed fluctuations of local electrostatic fields. This in turn can not happen unless the fluctuations of nearby hydrogen-bonded clusters (intra- and interclus-

ter fluctuations) become correlated as to maximize local field fluctuations while maintaining as many as possible mutual water arrangements close to the optimal HB geometry. Thus, in order to satisfy the *local energetic demand* to form hydrogen bonds, the resulting *entropic frustration relaxes non-locally* in the vicinity of a hydrophobic solute.

Testing this hypothesis demands the evaluation of various many-body correlations. Although addressing the problem of coupled translational-orientational multi-body correlations is nontrivial it can be significantly simplified in the following manner. While single water molecules are, by nature, indistinguishable they can be *transiently* classified as being hydrogen bonded or non-bonded to its nearest neighbor (using the same criteria as above). Any HB exchange event merely permutes the indices between water molecules. With these criteria we can, at any instant, classify the HB and non-HB neighbors of any given molecule. Involving various types of fluctuations on different time-scales, such as librations, dimer tumbling and HB jumping (see for example²⁶ and references therein), following both the relative positions and orientations of water molecules individually is simply too complex and in fact unnecessary. To determine how molecular degrees of freedom are constrained in the liquid state we shall be primarily interested in structural fluctuations in water clusters. Such fluctuations can be easily described in terms of fluctuations of interaction energies of hydrogen bonded and non-hydrogen bonded molecules.

Using the random variable transformation theorem²⁷ we can map the joint configurational probability density onto its functionally dependent joint probability density for pair potential energies. Thereby a given matrix of molecular positions and orientations, $\boldsymbol{\Omega}$, is mapped onto a vector of interaction energies, \mathbf{U} , which can be formally written for given values $\boldsymbol{\omega}$ and \mathbf{u} as follows:

$$p(\mathbf{u}) = \int d\boldsymbol{\omega}^N P(\boldsymbol{\omega}^N) \delta(\mathbf{u} - \mathbf{f}(\boldsymbol{\omega}^N)), \quad (2)$$

The functional relation $\delta(\mathbf{u} - \mathbf{f}(\boldsymbol{\omega}^N))$ contains a class indicator (close contact, hydrogen-bonded, etc.) as well as the appropriate averaging operation accounting for the indistinguishability of pairs within a certain class (for details see section 1 in the Supplementary information). This way we can construct, using appropriate functional relations, probability densities for observing, for example, a (non)hydrogen bonded pair with certain energy or a joint probability density of observing two pairs of different classes having given energies. Comparing the values per water molecule/cluster inside the first and second hydration shell with the corresponding bulk values we are able to select the most important contributions

to the entropy loss. The Gibbs-Shannon entropy, $S[p] = -k_B \int p(u_i) \ln p(u_i) du_i$, is used to evaluate the total uncertainty of a quantity u_i , and thus quantifies the fluctuations. Alternatively, Kullback-Liebler entropy or *Correlation entropy* (the latter is taken after²⁸) is used to quantify the total correlation between two random variables X and Y (which can be components of \mathbf{U} , for example various combinations of hydrogen-bonded and non-HB pairs (U_{HB} and U_{non-HB})). The correlation entropy can be expressed in terms of individual and joint entropies, $S_C(X, Y) = S(X) + S(Y) - S(X, Y)$, or explicitly in terms of corresponding probability densities:

$$S_c(X, Y) = k_B \iint p(x, y) \ln \frac{p(x, y)}{p(x)p(y)} dx dy. \quad (3)$$

We limit the present discussion to 3 and 4-particle correlations to assess how fluctuations of various HB and non-HB pairs are correlated.

Being predominantly interested in generic features and less on the specific effect of solute sizes we focus first on the properties of individual pairs of molecules and find that the dipolar entropy difference between the hydration shells and the bulk, which directly measures the degree of orientational constraining, does not show a monotonic behavior with respect to the solute size and is less than 1% of the corresponding bulk value (for details see section 2 in the Supplementary information). This confirms the assumptions that a reduced orientational configuration space of single molecules is *not* the reason for HE. This fact is further substantiated with the values of the entropy difference, ΔS_{tot-c} , of the fluctuations of the total interaction energy of tagged molecules with its nearest neighbors, $S[p(\sum_i U_{i0})]$, (Fig 3a). It may also be taken as a contribution to the fluctuations of the local electrostatic field (solely) due to the thermal motion of nearest neighbors. In fact, ΔS_{tot-c} is mostly positive, except for the smallest solute which indicates that local field fluctuations due to nearest neighbors are enhanced in the vicinity of the hydrophobe. Meanwhile, the entropy of mutual fluctuations of the potential energy of both hydrogen bonded neighbor pairs (Fig. 3a blue) and non-hydrogen bonded pairs (Fig. 3a green) decrease with respect to bulk water. The former can be understood as a measure of librational-type of fluctuations and its lowering is indicative of a slight HB strengthening²⁴ (though the relative difference is smaller than 2% of the bulk value). Together with decreasing fluctuations of the non-HB interaction energy and the simultaneous increase of fluctuations of the total interaction energy with nearest neighbors this immediately hints at higher order (beyond pair) correlations, as suggested

by our hypothesis. The local strengthening of HB is also suggested by the shift of $p(D)$ towards larger D . The fact that fluctuations of the total interaction energy are so small and their entropy difference mostly even positive along with the strengthening of HB are fully consistent with the large-amplitude sudden jump picture of HB-network dynamics. A closer look at entropies of various 3- and 4-body correlations in Fig 3b-d reveals striking, upto 22 fold increases with respect to bulk water. The largest increase is observed in the case of correlations of nearby non-HB pairs bridged via a HB (12-22 fold), a HB pair and a nearby non-HB pair (7-9 fold 9-15 in the case of geminal and 9-15 fold in the case of vicinal pairs) and two HB pairs that do not share a common HB bond (are not bridged via a HB; 9-11 fold). A significant, albeit smaller, increase is also observed in the case of geminal HB pairs (app. 100% increase) and HB pairs which are bridged via a HB (70-90% increase). Let us briefly mention that all 3- and 4-body correlations are, to linear order, anti-correlated. The pronounced many-body correlations propagate into the second hydration shell (for details see Table 1 in section 3 of the Supplementary information) but fall off rapidly further away. Thus, the picture of two perturbed hydration layers is retained.

The results suggest that the traditional explanation of the HE on the molecular scale needs a substantial revision. It is not a reduced configuration space for hydrogen bonding that is responsible for the observed lowering of entropy, but a striking increase of many-body correlations (Fig. 4a), which is essentially due to hydrogen bonding being a strong and orientationally dependent interaction. The increase of many-body correlations is necessary to compensate for the reduction of fluctuations in the local electrostatic field and the resulting local HB-strengthening when one or more "polar" water molecules are replaced by an "apolar" hydrophobic particle. This effect should scale as the difference between local field distributions experienced by the water molecule in bulk (Fig. 4b black curve) and by a bulk water molecule for which one neighboring water molecule is omitted from the calculation of the local field (Fig. 4b black curve). If left uncompensated, such as in the latter case, the distribution is shifted significantly to lower values. It also turns out that the distributions of field strengths in the hydration shells are almost identical to the one in bulk liquid (Fig. 4b symbols). Furthermore, by looking at the distribution of orientations of the local field over the unit sphere (for details see Fig. 4c and section 2 of the Supplementary information) shown in Figure 4d we find that the distribution is isotropic in the bulk as well as in the second hydration shell (not shown). Meanwhile, in the first hydration shell the local field

fluctuations are constrained to the plane containing the normal to the solute surface. Such a distribution ensures that all water molecules in the first hydration shell experience the maximum span of local fields and thereby local torques which counteract the entropic frustrations caused by a transient mutual alignment of water molecules in between HB exchange events. Such a compensation mechanism comes at cost of many-body correlations. The local increased entropic frustration is thus compensated non-locally.

The proposed picture of hydrophobic hydration does not imply any water immobilization in the spirit of the iceberg hypothesis. In explaining the moderate retardation of reorientation dynamics^{23,30} the current picture, based on the excluded volume effect, proposes that the slowdown is a result of fewer accessible configurations of the transition-state (TS) in a HB exchange event due to the presence of the solute. We demonstrate that the lower number of accessible TS configurations rather results from many-body correlations (*due to correlations the TS is simply statistically less probable*) rather than actual sterical hindrance of reorientation. Thus the expression for the slowdown factor remains unaffected. Our view also provides an explanation of the slightly better solubility of nonpolar solutes in heavy relative to light water³¹. While being more inert heavy water responds less strongly to local field fluctuations, which leads to HB strengthening and thus a higher cohesive energy density³¹ but also results in a more structured liquid with respect to light water³². Being intrinsically more structured the relative extent of local field fluctuations to be compensated upon the introduction of a hydrophobic molecule is therefore also smaller.

Finally, the results allow us to speculate that the range of hydrophobic interactions beyond that expected from the minimally-exposed surface area reasoning is a result of the propagation of many-body correlations beyond the first hydration shell.

I. METHODS

We performed extensive constant pressure Monte-Carlo (MC) simulations with TIP5P water and freely moving hard sphere solutes at room temperature (298 K) and 1 atm assuming periodic boundary conditions. After an extensive equilibration period we performed as many trial moves as to assure that on average each molecule was *successfully* moved 4×10^5 times at the maintained acceptance rate of 30%. To exclude (auto)correlations the successive configurations used for the analysis were taken to be as far apart as to assure that between

each taken configuration each molecule was *successfully* moved at least 5 times. The hard sphere radius of the water molecule when in close contact with the hydrophobic spheres was taken to be 1.4 Å. The following radii of solutes were considered: $r(s1)=1.4$ Å, $r(s2)=2.1$ ($1.5 \times r_{H_2O}^{hs}$) Å, $r(s3)=2.52$ ($1.8 \times r_{H_2O}^{hs}$) Å and $r(s4)=2.8$ ($2 \times r_{H_2O}^{hs}$) Å. According to the solute size the number of water molecules was (in ascending size) 2668, 2670, 3513 and 3560. The total number of MC steps was 35.57×10^8 , 35.60×10^8 , 46.8×10^8 and 47.5×10^8 .

II. REFERENCES

* aljaz.godec@ki.si

† franci.merzel@ki.si

- ¹ Chandler, D. Interfaces and the driving force of hydrophobic assembly. *Nature* **437**, 640-647 (2005).
- ² Lum, K., Chandler, D., Weeks, J. D. Hydrophobicity at small and large length scales. *J. Phys. Chem B* **103**, 4570-4577 (1999).
- ³ Rajamani, S. Truskett, T. M., Garde, S. Hydrophobic hydration from small to large lengthscales: Understanding and manipulating the crossover. *Proc. Natl. Acad. Sci. USA* **102**, 9475-9480 (2005).
- ⁴ Mittal, J., Hummer, G. Static and dynamic correlations in water at hydrophobic interfaces. *Proc. Natl. Acad. Sci. USA* **105**, 20130-20135 (2008).
- ⁵ Huang, D. M., Chandler, D. Temperature and length scale dependence of hydrophobic effects and their possible implications for protein folding. *Proc. Natl. Acad. Sci. USA* **97**, 8324-8327 (2000).
- ⁶ Papoian, G. A., Ulander, J., Eastwood, M. P., Luthey-Schulten, Z., Wolynes, P. G. Water in protein structure prediction. *Proc. Natl. Acad. Sci. USA* **101**, 3352-3357 (2004).
- ⁷ Rabani, E., Reichman, D. R., Geissler, P. L., Brus, L. E. Drying-mediated self-assembly of nanoparticles. *Nature* **426**, 271-274 (2003).
- ⁸ Stillinger, F.H. Water revisited. *Science* **20**, 451-457 (1980).

- ⁹ Murthy, K. P., Privalov, P. L., Gill, S. J. Common features of protein unfolding and dissolution of hydrophobic compounds. *Science* **247**, 559-561 (1990).
- ¹⁰ Lynden-Bell, R. M., Giovambattista, N., Debenedetti, P. G., Head-Gordon, T., Rossky, P. J. Hydrogen bond strength and network structure effects on hydration of non-polar molecules. *Phys. Chem. Chem. Phys.* **13**, 2748-2757 (2011).
- ¹¹ Pratt, L.R. Colloquium: Scaled particle theory and the length scales of hydrophobicity. *Rev. Mod. Phys.* **78**, 159178 (2006).
- ¹² Hummer, G., Garde, S., Garcia, A. E., Pohorille, A., Pratt, L. R. An information theory model of hydrophobic interactions. *Proc. Natl. Acad. Sci. USA* **93**, 8951-8955 (1996).
- ¹³ Tanford, C. The hydrophobic effect and the organization of living matter. *Science* **200**, 1012-1018 (1978).
- ¹⁴ Ben-Naim, B. *Hydrophobic Interactions* (Plenum, New York, 1980).
- ¹⁵ Pratt, L.R. MOLECULAR THEORY OF HYDROPHOBIC EFFECTS: 'She is too mean to have her name repeated.' *Ann. Rev. Phys. Chem.* **53**, 409-436 (2002).
- ¹⁶ Bowron, D. T., Filipponi, A., Roberts, M. A., Finney, J. L. Hydrophobic Hydration and the Formation of a Clathrate Hydrate. *Phys. Rev. Lett.* **81**, 4164-4167 (1998).
- ¹⁷ Chatterjee, S., Debenedetti, P. G., Stillinger, F. H., Lynden-Bell, R. M. A computational investigation of thermodynamics, structure, dynamics and solvation behavior in modified water models. *J. Chem. Phys.* **128**, 124511-9 (2008).
- ¹⁸ Mahoney, M. W., Jorgensen, W. L. A five-site model for liquid water and the reproduction of the density anomaly by rigid, nonpolarizable potential functions. *J. Chem. Phys.* **112**, 8910-8922 (2000).
- ¹⁹ Laage, D., Hynes, J.T. A molecular jump mechanism of water reorientation. *Science* **311**, 832-835 (2006).
- ²⁰ Godec, A., Smith, J.C., Merzel, F. Increase of both order and disorder in first hydration shell upon increasing solute polarity. *Phys. Rev. Lett.*, accepted for publication (2011).
- ²¹ Laage, D., Hynes, J.T. On the Molecular Mechanism of Water Reorientation. *J. Phys. Chem. B* **112**, 1423014242 (2008).
- ²² Eaves, J.D., Loparo, J.J., Fecko, C.J., Roberts, S.T., Tokmakoff, A., Geissler, P.L. Hydrogen bonds in liquid water are broken only fleetingly. *Proc. Natl. Acad. Sci. USA* **102**, 13019-13022 (2005).

- ²³ Laage, D. Reinterpretation of the liquid water quasi-elastic neutron scattering spectra based on a nondiffusive jump reorientation mechanism. *J. Phys. Chem. B* **113**, 26842687 (2009).
- ²⁴ Moilanen, D.E., Wong, D., Rosenfeld, D.E., Fenn, F.E., Fayer, M.D. Ion-water hydrogen-bond switching observed with 2D IR vibrational echo chemical exchange spectroscopy. *Proc. Natl. Acad. Sci. USA* **106**, 375-380 (2009).
- ²⁵ Ji, M., Odellius, M., Gaffney, K.J. Large angular jump mechanism observed for hydrogen bond exchange in aqueous perchlorate solution. *Science* **328**, 1003-1005 (2010).
- ²⁶ Laage, D., Stirnemann, G., Sterpone, F., Rey, R., Hynes, J. Reorientation and allied dynamics in water and aqueous solutions. *Annu. Rev. Phys. Chem.* **62**, 395-416 (2011).
- ²⁷ Gillespie, D.T. A theorem for physicists in the theory of random variables. *Am. J. Phys.* **51**, 520-533 (1983).
- ²⁸ Gu, S.J., Sun, C.P., Lin, H.Q. Universal role of correlation entropy in critical phenomena. *J. Phys. A: Math. Theor.* **41**, 024002 (18pp) (2008).
- ²⁹ Moilanen, et al. Water inertial reorientation: hydrogen bond strength and the angular potential. *Proc. Natl. Acad. Sci. USA* **105**, 5295-5300 (2008).
- ³⁰ Qvist, J., Halle, B. Thermal signature of hydrophobic hydration dynamics. *J. Am. Chem. Soc.* **130**, 10345-10353 (2008).
- ³¹ Graziano, G. Relationship between cohesive energy density and hydrophobicity. *J. Chem. Phys.* **121**, 1878-1882 (2004).
- ³² Soper, A.K., Benmore, C.J. Quantum differences between heavy and light water. *Phys. Rev. Lett.* **101**, 065502-1-4 (2008).

III. ACKNOWLEDGEMENTS

We thank U. Maver for his help in preparation of schematics and professors M. R. Johnson, M. Gaberšček and P. Zihlerl for suggestions and critical reading of the manuscript.

Figure 1: **Radial ordering around hydrophobic particles.** **a** Radial correlation function for water centers; (inset) corresponding relative density fluctuations. (bottom) Distribution of the number of total (dashed lines) and hydrogen-bonded (full lines) contacts per water molecule located in the **b** first and **c** second hydration shell with the corresponding bulk water values for comparison. The vertical lines denote expected values. The solute sizes are: $r(s1)=1.4 \text{ \AA}$, $r(s2)=2.1 (= 1.5 \times r_{H_2O}^{hs}) \text{ \AA}$, $r(s3)=2.52 (= 1.8 \times r_{H_2O}^{hs}) \text{ \AA}$ and $r(s4)=2.8 (= 2 \times r_{H_2O}^{hs}) \text{ \AA}$ (see Methods for details).

Figure 2: **Mutual orientational ordering of water molecules in close contact.** Difference in the distribution of the dipolar order parameter with respect to the bulk, $\Delta p(D) = p(D) - p_B(D)$, in the first **a** and second **b** hydration shell. The dipolar order distribution in bulk water is shown in the inset of **a**. **c** Joint probability of finding two molecules at a distance r apart having a (pair) mutual order D_2 (see Eq. 1 for definition, with $N=1$).

Figure 3: **Fluctuation and correlation entropy differences per tagged pair/cluster in the first hydration shell with respect to the bulk are given in the Tables. Correlations between differently interacting pairs of water molecules are depicted by colour in schematics and Tables.** Only the tagged molecule necessarily lies in the first hydration shell. The crosses denote the tagged molecule which is used for the localization of a given cluster and the dashed black lines denote HBs. **a** Absolute and relative entropy difference of fluctuations of HB (blue shading), non-HB (green shading) and total interaction energy with nearest neighbors (black frame). The slight increase of the entropy of total interaction energy fluctuations accompanied with the simultaneous decrease of entropy of HB and non-HB energy fluctuations is indicative of higher order correlations. **b** 3-body correlation entropy of geminal (pairs share the tagged molecule) HB pairs (blue shading) and a geminal HB and non-HB pair (black frame). **c** 4-body correlation entropy of HB-bridged HB pairs (blue shading), non-HB-bridged HB pairs (black frame) and a vicinal (pairs do not share the tagged molecule) tagged HB and non-HB pair (magenta frame). **d** 4-body correlation entropy of vicinal HB-bridged non-HB pairs (green shading), vicinal

non-HB-bridged non-HB pairs (magenta frame) and a vicinal tagged non-Hb and HB pair (black frame). The upto 2200% increase of many-body correlations with respect to bulk water confirms their crucial role in mediating the hydrophobic effect.

Figure 4: **Emergence of pronounced many-body correlations and their physical origin.** **a** In bulk water the fluctuations are correlated predominantly up to the pair level. In the vicinity of hydrophobic solutes significant many-body correlations emerge in order to compensate for reduced fluctuations in the local electrostatic field as a result of the exceedingly small field of the hydrophobic solute. Different colours denote various orders of correlated fluctuations. **b** Distribution of magnitudes of the local electrostatic field experienced by a water molecule at a given location. Black lines denote distributions in bulk water and symbols represent results for water molecules around apolar solute. If one nearest neighbor water molecule is omitted from the calculation of the local field in the bulk, this leads to uncompensated fluctuations shown by the red distribution. Results are given as relative deviations from the average bulk value $|\overline{\mathbf{E}_b}|$. Note that the strength of the local field experienced by water molecules in the first and second hydration shell is almost identical to the one in bulk water. **c** The coordinate frame used in the calculation of angular distributions of local electrostatic fields. The radial projection of the water molecule position onto a spherical surface (θ', φ') defines the origin and orientation of a secondary coordinate system (blue), such that the secondary $z(\theta', \varphi')$, $\mathbf{x}(\theta', \varphi')$ and $\mathbf{y}(\theta', \varphi')$ axes correspond to the local radial, polar and azimuthal directions. Angular coordinates in the secondary frame $(\theta\{\theta', \varphi'\}, \varphi\{\theta', \varphi'\})$ are used to describe the distribution of the local field over the surface of the unit sphere. **d** Distribution of orientations of the local electrostatic field in the first hydration shell of apolar solutes and in bulk water. In the first hydration shell the orientational fluctuations of the local field are confined to the plane containing the normal to the solute surface. The distribution in the bulk as well as in the second hydration shell (not shown) is entirely isotropic.

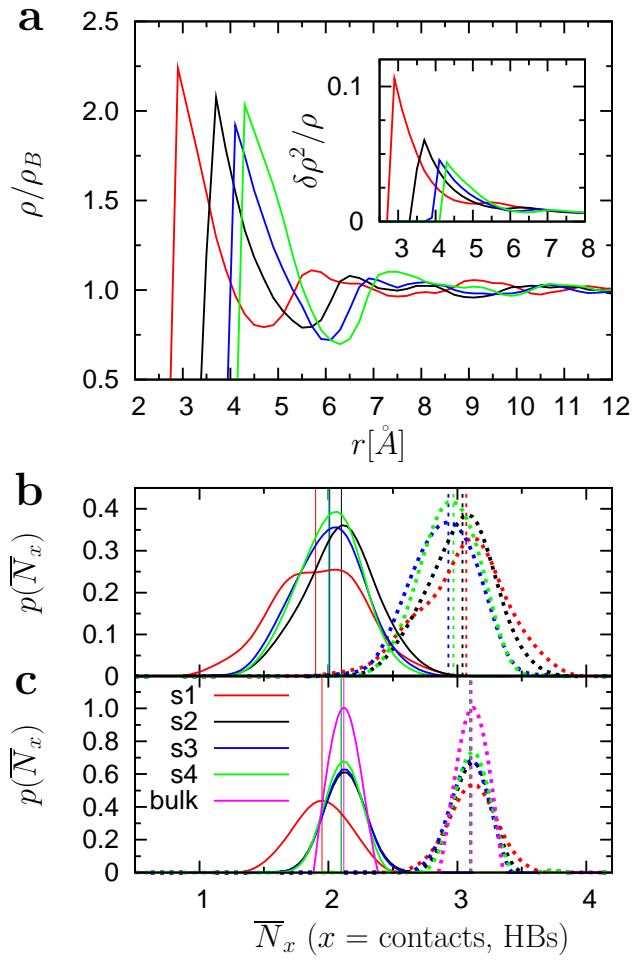


FIG. 1.

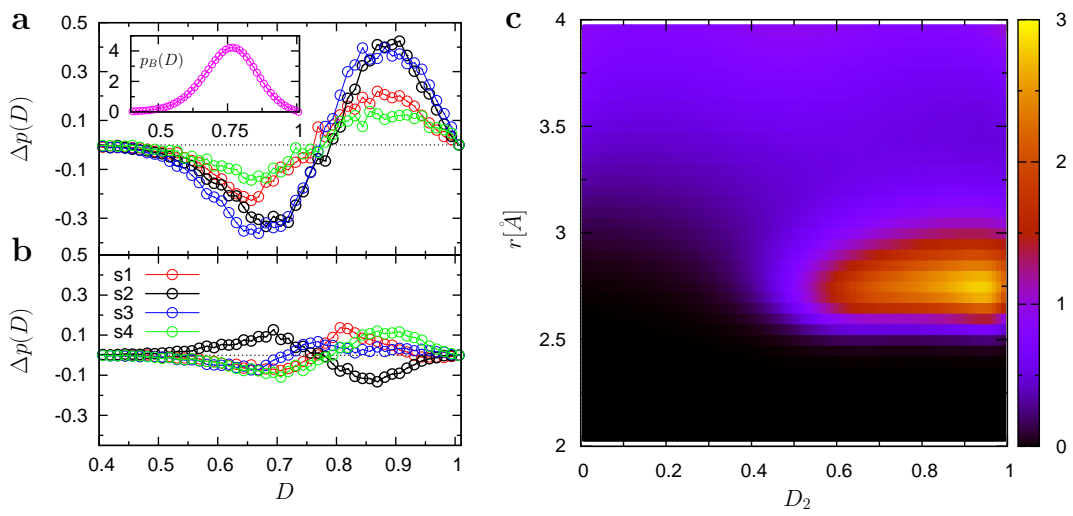


FIG. 2.

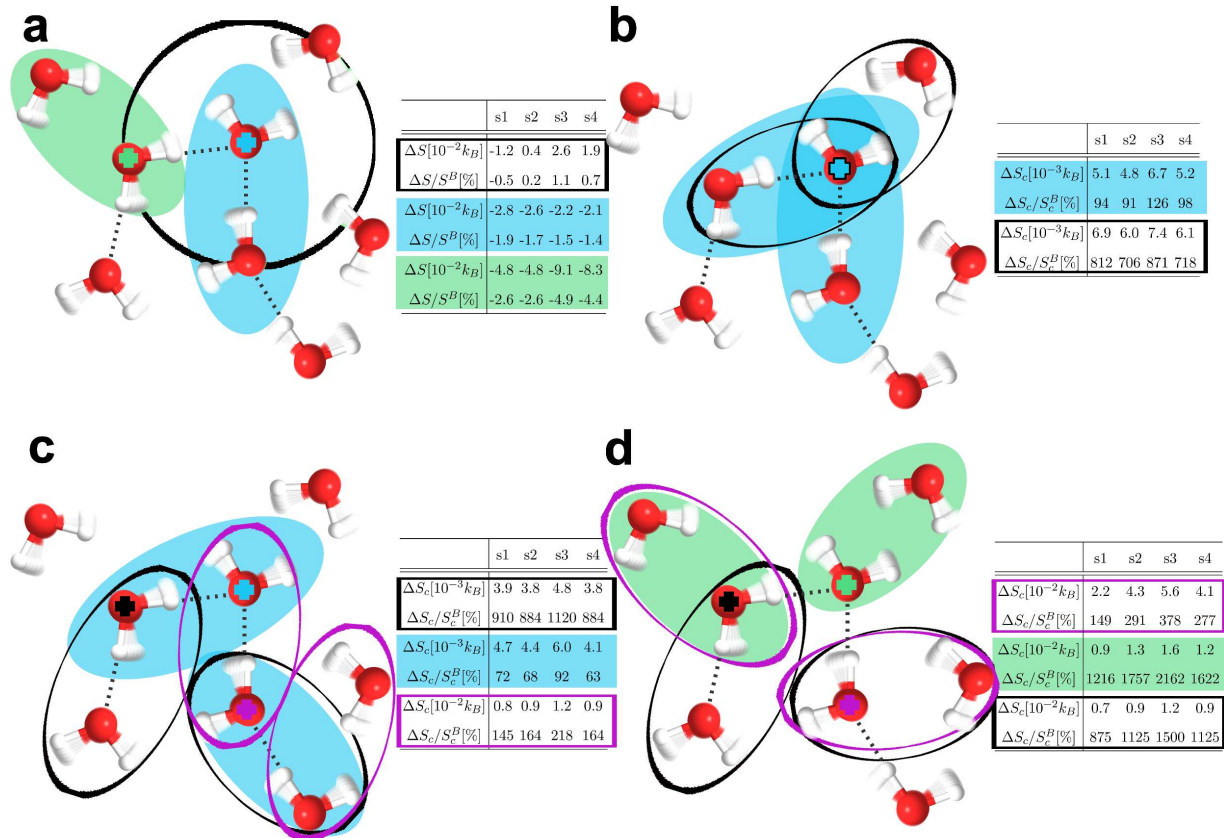


FIG. 3.

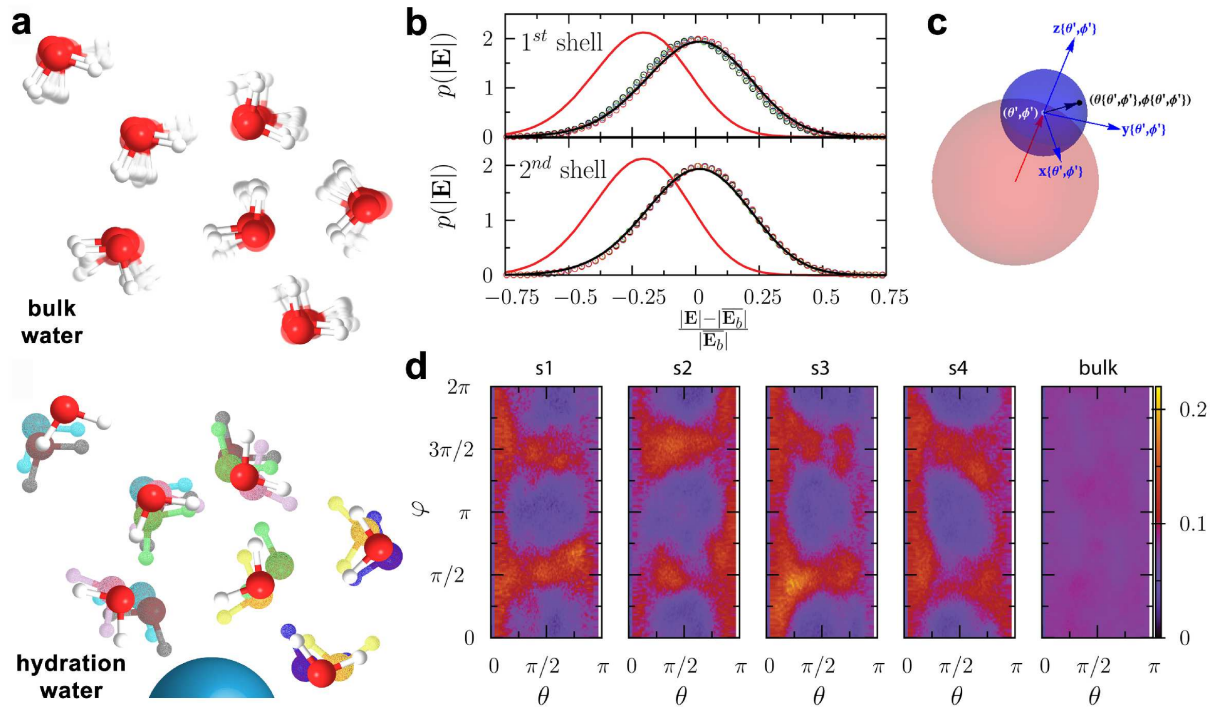


FIG. 4. Fig 4

Supplementary information for: Physical origin underlying the entropy loss upon hydrophobic hydration

Aljaž Godec^{1,*} and Franci Merzel^{1,†}

¹*National Institute of Chemistry, Hajdrihova 19, 1000 Ljubljana, Slovenia*

(Dated: June 18, 2018)

* aljaz.godec@ki.si

† franci.merzel@ki.si

I. PROBABILITY DENSITIES AND THE MAPPING ONTO POTENTIAL ENERGY SPACE

Throughout the paper as well as this section we strictly discriminate between a random variable, which is denoted by uppercase letters, and a value it can take on (lowercase letters). The random variable transformation theorem is used to map the joint configurational probability density, onto its functionally dependent joint probability density for pair potential energies. Thereby molecular positions and orientations, $\boldsymbol{\Omega}^N = (\mathbf{R}^N, \boldsymbol{\alpha}^N)$, are mapped onto a vector of interaction energies, \mathbf{U} :

$$p(\mathbf{u}) = \int d\boldsymbol{\omega}^N P(\boldsymbol{\omega}^N) \delta(\mathbf{u} - \mathbf{f}(\boldsymbol{\omega}^N)), \quad (1)$$

The functional relation $\delta(\mathbf{u} - \mathbf{f}(\boldsymbol{\omega}^N))$ contains class indicators (close contact, hydrogen-bonded, etc.) and the appropriate averaging operation accounting for the indistinguishability of pairs within a certain class.

If we denote the solute position as \mathbf{R}_s the general functional expressions $\delta(\mathbf{u} - \mathbf{f}(\boldsymbol{\omega}^N))$ can be written as follows.

In the scalar case (*i.e.* density $p(U_x)$) we have:

$$\delta(u - f(\boldsymbol{\omega}^N)) \equiv \frac{\sum_{i,j \neq i} \delta(u - u(\boldsymbol{\omega}_i, \boldsymbol{\omega}_j)) \chi_d(\boldsymbol{\omega}_i, \boldsymbol{\omega}_j) \chi_{HB}(\boldsymbol{\omega}_i, \boldsymbol{\omega}_j) \Pi_{R_{min}, R_{max}}(|\mathbf{r}_i - \mathbf{r}_s|)}{\int d\boldsymbol{\omega}^N P(\boldsymbol{\omega}^N) \left\{ \sum_{i,j \neq i} \chi_d(\boldsymbol{\omega}_i, \boldsymbol{\omega}_j) \chi_{HB}(\boldsymbol{\omega}_i, \boldsymbol{\omega}_j) \Pi_{R_{min}, R_{max}}(|\mathbf{r}_i - \mathbf{r}_s|) \right\}} \quad (2)$$

where $\chi_d(\boldsymbol{\Omega}_i, \boldsymbol{\Omega}_j)$ is the indicator function for the distance cutoff for nearest neighbors

$$\chi_d(\boldsymbol{\omega}_i, \boldsymbol{\omega}_j) \equiv (1 - H(|\mathbf{r}_i - \mathbf{r}_j|)), \quad (3)$$

$H(x)$ being the Heaviside function and $\chi_{HB}(\boldsymbol{\omega}_i, \boldsymbol{\omega}_j)$ is the indicator function for hydrogen bonding (which is left out in the case of non-hydrogen bonded neighbors)

$$\chi_{HB}(\boldsymbol{\omega}_i, \boldsymbol{\omega}_j) \equiv H(\vartheta[OH_i \cdots O_j] - \vartheta_{min}) + H(\vartheta[OH_j \cdots O_i] - \vartheta_{min}), \quad (4)$$

where $\vartheta[OH_i \cdots O_j]$ is the angle between the OH bond of the donor molecule and vector connecting the proton of the donor molecule and the acceptor oxygen. ϑ_{min} is the lower cutoff for the hydrogen bonding angle. $\Pi_{a,b}(x)$ represents the boxcar function

$$\Pi_{R_{min}, R_{max}}(|\mathbf{r}_i - \mathbf{r}_s|) \equiv \begin{cases} 0 & \text{if } |\mathbf{r}_i - \mathbf{r}_s| < R_{min}, \\ 1 & \text{if } R_{min} \leq |\mathbf{r}_i - \mathbf{r}_s| \leq R_{max}, \\ 0 & \text{if } |\mathbf{r}_i - \mathbf{r}_s| > R_{max}. \end{cases} \quad (5)$$

which localizes the tagged molecule i in a certain hydration shell (first, second shell or bulk).

In the non-scalar case $p(\mathbf{U})$ is a joint distribution. Then we have, for example for a joint distribution for a 3-body or 4-body density (or equivalently for a pair density of pairs), $p(U_{0x}, U_{0y})$ or $p(U_{0x}, U_{jz})$ respectively:

$$\delta(\mathbf{u} - \mathbf{f}(\boldsymbol{\omega}^N)) \equiv \frac{\sum_{ijkl} \delta(u - u^{ij}) \delta(u - u^{kl}) \chi_d^{ij} \chi_d^{kl} \chi_{HB}^{ij} \chi_{HB}^{kl} \Pi_{R_{min}, R_{max}}(d_i) (1 - \delta_{il} \delta_{jl} \delta'_{ik} \delta_{jk}) \Theta_c^{ijkl}}{\int d\boldsymbol{\omega}^N P(\boldsymbol{\omega}^N) \left\{ \sum_{ijkl} \chi_d^{ij} \chi_d^{kl} \chi_{HB}^{ij} \chi_{HB}^{kl} \Pi_{R_{min}, R_{max}}(d_i) (1 - \delta_{il} \delta_{jl} \delta'_{ik} \delta_{jk}) \Theta_c^{ijkl} \right\}}, \quad (6)$$

where the explicit coordinate dependences $(\boldsymbol{\Omega}_i, \boldsymbol{\Omega}_j)$ were replaced by superscripts ij , $d_i = |\mathbf{r}_i - \mathbf{r}_s|$ and δ_{ij} is the Kronecker delta. The primed Kronecker delta denotes that i may or may not be equal to k , depending on whether we take geminal or vicinal pairs of molecules, that is, 3- or 4- particle correlations (for the explicit definition of geminal and vicinal pairs see main text). For geminal pairs the primed Kronecker delta is omitted. Θ_c^{ijkl} is the connectivity indicator function and defines the topological relation between both pairs. Two pairs may be connected with a hydrogen bond or not.

Corresponding equation for higher dimensional probability densities can be constructed accordingly.

II. CALCULATION OF THE ORIENTATIONAL DISTRIBUTION OF THE LOCAL ELECTROSTATIC FIELD

The systems under investigation all have spherical symmetry around the center of the solute. Thus, all points in the space-fixed frame (denoted by prime) with the same radius r' are positionally equivalent. As we classify the water molecules according to their position with respect to the solute as belonging to the first and second hydration shell or the bulk, we can drop the radial component when dealing with molecules in a particular shell and simply retain the angular variables (θ', φ') , where $\theta' = \arccos(\frac{z'}{r'})$ and $\varphi' = \arctan(\frac{y'}{x'})$. We choose to describe the orientational distribution of the instantaneous electrostatic field orientation in a given point of the space-fixed frame as a distribution over the surface of a unit sphere. In order to take into account the equivalence of positions at given radius in the space-fixed frame we set the secondary local frame in the following manner. The secondary x, y and z axes are chosen to coincide with the polar, azimuthal and radial directions at

(θ', φ') . Specifically, this amounts to the following basis:

$$\hat{\mathbf{x}}(\theta', \varphi') = \begin{pmatrix} \cos \varphi' \sin \theta' \\ \sin \varphi' \cos \theta' \\ -\sin \theta' \end{pmatrix}, \quad \hat{\mathbf{y}}(\theta', \varphi') = \begin{pmatrix} -\sin \varphi' \\ \cos \varphi' \\ 0 \end{pmatrix}, \quad \hat{\mathbf{z}}(\theta', \varphi') = \begin{pmatrix} \cos \varphi' \sin \theta' \\ \sin \varphi' \sin \theta' \\ \cos \theta' \end{pmatrix}.$$

The local electrostatic field at a point $\mathbf{r}' = (x', y', z')$ due to a collection of N point charges q_i with coordinates \mathbf{r}''_i is $\mathbf{E}(\mathbf{r}') = \sum_{i=1}^N \frac{q_i(\mathbf{r}' - \mathbf{r}''_i)}{|\mathbf{r}' - \mathbf{r}''_i|^3}$. The unit Cartesian components of the field in the secondary frame at (r', θ', φ') are thus:

$$\hat{E}_x(r', \theta', \varphi') = \frac{(\mathbf{E}(\mathbf{r}') \cdot \hat{\mathbf{x}})}{|\mathbf{E}(\mathbf{r}')|}, \quad \hat{E}_y(r', \theta', \varphi') = \frac{(\mathbf{E}(\mathbf{r}') \cdot \hat{\mathbf{y}})}{|\mathbf{E}(\mathbf{r}')|}, \quad \hat{E}_z(r', \theta', \varphi') = \frac{(\mathbf{E}(\mathbf{r}') \cdot \hat{\mathbf{z}})}{|\mathbf{E}(\mathbf{r}')|}.$$

After a trivial transformation to spherical coordinates in the secondary frame, we may write for the orientational distribution of the electrostatic field experienced by a water molecule in shell d_i (first, second or bulk):

$$p(\theta, \varphi)[d_j] = \left\langle \frac{\sum_{i=1}^N \delta(\hat{E}_{\theta,i} - \theta) \delta(\hat{E}_{\varphi,i} - \varphi) \Pi_{R_{min}, R_{max}}(d_i)}{\sum_{i=1}^N \Pi_{R_{min}, R_{max}}(d_i)} \right\rangle.$$

III. GIBBS-SHANON AND CORRELATION ENTROPY DIFFERENCES

We denote a tagged molecule with 0, its neighbors with $i, j, k; i \neq j \neq k \neq \dots$, and the nearest neighbors of the nearest neighbors with primes. A 3-body correlation entropy of a tagged molecule and its two nearest HB neighbors is thus, for example, S_{HB-HB}^{i0-0j} , and the 4-body correlation entropy of two adjacent HB pairs is $S_{HB-HB}^{i0-jk'}$, if j is not hydrogen-bonded to 0, and $S_{HB-HB}^{i0-jk'^*}$, if j is a HB neighbor of 0. .

TABLE I. Entropy differences per water molecule in the first and second shell for various solute sizes. ΔS_i stands for $S^i - S_B^i$ and the asterisk denotes that molecule j is hydrogen-bonded to the tagged molecule 0.

	s1 1 st	s1 2 nd	s2 1 st	s2 2 nd	s3 1 st	s3 2 nd	s4 1 st	s4 2 nd
$\Delta S_D[10^{-3}k_B]$	-7.9	-6.4	4.5	2.0	-4.6	-6.1	5.6	3.3
$\Delta S_D/S_D^B[10^{-1}\%]$	8.6	6.9	-4.9	-2.2	5.0	6.7	-6.2	-3.6
$\Delta S_{tot-c}[10^{-2}k_B]$	-1.2	-0.3	0.4	0.2	2.6	-0.3	1.9	0.2
$\Delta S_{tot-c}/S_{tot-c}^B[\%]$	-0.5	-0.1	0.2	0.1	1.1	-0.1	0.7	0.1
$\Delta S_{HB}[10^{-2}k_B]$	-2.8	-1.1	-2.6	0.4	-2.2	0.07	-2.1	-0.5
$\Delta S_{HB}/S_{HB}^B[\%]$	-1.9	-0.7	-1.7	0.3	-1.5	0.05	-1.4	0.3
$\Delta S_{nHB}[10^{-2}k_B]$	-4.8	-0.5	-4.8	-0.1	-9.1	-0.3	-8.3	-0.9
$\Delta S_{nHB}/S_{nHB}^B[\%]$	-2.6	-0.3	-2.6	-0.05	-4.9	-0.16	-4.4	-0.5
$\Delta S_{HB-HB}^{i0-0j}[10^{-3}k_B]$	5.1	1.7	4.8	1.3	6.7	1.9	5.2	1.8
$\Delta S_{HB-HB}^{i0-0j}/S_{HB-HB}^{i0-0j;B}[\%]$	94	31	91	25	126	36	98	34
$\Delta S_{HB-nHB}^{i0-0j}[10^{-3}k_B]$	6.9	2.0	6.0	1.8	7.4	2.2	6.1	1.7
$\Delta S_{HB-nHB}^{i0-0j}/S_{HB-nHB}^{i0-0j;B}[\%]$	812	235	706	212	871	256	718	200
$\Delta S_{HB-HB}^{i0-jk'}[10^{-3}k_B]$	3.9	1.2	3.8	1.1	4.8	1.3	3.8	1.1
$\Delta S_{HB-HB}^{i0-jk'}/S_{HB-HB}^{i0-jk';B}[\%]$	910	440	884	260	1120	320	884	256
$\Delta S_{HB-HB}^{i0-jk'^*}[10^{-3}k_B]$	4.7	1.2	4.4	0.9	6.0	1.4	4.1	1.4
$\Delta S_{HB-HB}^{i0-jk'^*}/S_{HB-HB}^{i0-jk'^*;B}[\%]$	72	18	68	14	92	22	63	22
$\Delta S_{nHB-nHB}^{i0-jk'}[10^{-2}k_B]$	2.2	0.6	4.3	1.1	5.6	1.3	4.1	0.9
$\Delta S_{nHB-nHB}^{i0-jk'}/S_{nHB-nHB}^{i0-jk';B}[\%]$	149	41	291	74	378	88	277	61
$\Delta S_{nHB-nHB}^{i0-jk'^*}[10^{-2}k_B]$	0.9	0.3	1.3	0.3	1.6	0.4	1.2	0.3
$\Delta S_{nHB-nHB}^{i0-jk'^*}/S_{nHB-nHB}^{i0-jk'^*;B}[\%]$	1216	405	1757	405	2162	541	1622	405
$\Delta S_{HB-nHB}^{i0-jk'}[10^{-2}k_B]$	0.7	0.2	0.9	0.2	1.2	0.3	0.9	0.2
$\Delta S_{HB-nHB}^{i0-jk'}/S_{HB-nHB}^{i0-jk';B}[\%]$	875	250	1125	250	1500	375	1125	250
$\Delta S_{HB-nHB}^{i0-jk'^*}[10^{-2}k_B]$	0.8	0.2	0.9	0.2	1.2	0.3	0.9	0.3
$\Delta S_{HB-nHB}^{i0-jk'^*}/S_{HB-nHB}^{i0-jk'^*;B}[\%]$	145	26	164	26	218	55	164	55